

Multipath characteristics of GPS signals as determined from the Antenna and Multipath Calibration System

Kwan-Dong Park^{1,4}, James L. Davis¹, Per O. J. Jarlemark^{1,5}, Pedro Elosegui¹, James E. Normandeau¹, Brian E. Corey², Arthur E. Niell², Charles E. Meertens³, and Victoria A. Andreatta³,

¹*Harvard-Smithsonian Center for Astrophysics, Cambridge, Massachusetts*

²*MIT Haystack Observatory, Westford, Massachusetts*

³*UCAR/UNAVCO, Boulder, Colorado*

⁴*Now at Korea Astronomy Observatory, South Korea*

⁵*Now at Swedish National Testing and Research Institute, Sweden*

BIOGRAPHY

Dr. Kwan-Dong Park received his Ph.D. in Aerospace Engineering at the University of Texas at Austin, and he currently works at Korea Astronomy Observatory as Senior Research Staff in GPS Research Group.

Dr. James L. Davis received his Ph.D. in Geophysics at MIT and currently is the director of Space Geodesy group at Harvard-Smithsonian Center for Astrophysics.

Dr. Per O. J. Jarlemark received his Ph.D. in Electrical Engineering at Chalmers University of Technology and currently works at Swedish National Testing and Research Institute, Boras, Sweden.

Dr. Pedro Elosegui received his Ph.D. in Physics at University of Granada and currently works at Harvard-Smithsonian Center for Astrophysics as Geodesist.

Mr. James E. Normandeau works at Harvard-Smithsonian Center for Astrophysics as GPS Network Coordinator.

Dr. Brian E. Corey received his Ph.D. in Physics at Princeton University and currently works at MIT Haystack Observatory as Research Scientist.

Dr. Arthur E. Niell received his Ph.D. in Applied Physics at Cornell University and currently works at MIT Haystack Observatory as Research Scientist.

Dr. Charles E. Meertens earned his Ph.D. in Geophysics at the University of Colorado at Boulder and currently works at UNAVCO Facility, University Corporation for Atmospheric Research, Boulder, Colorado.

Ms. Victoria A. Andreatta received her B.S. at the University of Colorado at Boulder, and currently works at UNAVCO Facility as Engineer I.

ABSTRACT

Geophysical applications of the Global Positioning System (GPS) for studies such as global sea level change and glacial isostatic adjustment require very high accuracy ($1 \text{ mm}\cdot\text{yr}^{-1}$) determinations of site velocity, especially of its vertical component. Despite the many efforts devoted by investigators to the calibration of site-specific errors, signal scattering and multipath remain an unsolved problem. We have developed an Antenna and Multipath Calibration System (AMCS) for characterizing site-specific GPS phase measurement errors. The system consists of a high-gain, multipath-free, 3-m diameter parabolic antenna, a test antenna, and two Trimble GPS receivers. There are two modes of operating the AMCS: Zero-baseline (ZBL) and AMCS modes. In ZBL-mode, the two receivers simultaneously record the signal from the test GPS antenna. In this operating mode, one can determine the receiver clock synchronization error and the phase biases for each satellite. Typical RMS accuracies of ZBL-mode phase residuals are sub-millimeter level, ranging from 0.4 to 0.7 mm. In the AMCS-mode, one GPS receiver records the signal received at the test antenna, and the other records the signal from the parabola. Thus, one can compare the phases from the two receivers, and determine the antenna and multipath calibration errors of the test antenna. In our test cases with the test antenna located in a multipath-rich environment, the phase residuals obtained by tracking the same satellite over several days show large amplitude variations over small elevation angle ranges with highly repeatable patterns. The amplitude is 4-6 mm for low elevation angles and 1-2 mm for high elevation angles. Modeling

and subtracting the repeating patterns from the phase residuals results in RMS of about 1 mm. We have recently installed a second GPS antenna at a nearby location where the multipath effects are presumably less significant than at the location of the first GPS antenna. To further reduce multipath effects, all-weather microwave absorbers surrounded the second antenna. The amplitude of the phase residuals obtained for the second antenna location is significantly smaller than for the first antenna, implying that the second antenna is less affected by multipath. These independent results also served to confirm that the origin of the phase patterns measured is multipath.

INTRODUCTION

Two important error sources for precise geodesy with GPS are phase multipath [e.g., *Axelrad et al.*, 1996; *Byun et al.*, 2002] and direction-dependent variations in the antenna phase center [e.g. *Rothacher et al.*, 1995; *Mader and MacKay*, 1996]. (Geodetic applications generally utilize the carrier-beat phase as the primary GPS observable [e.g. *Segall and Davis*, 1997].) Both these problems stem from the basic design of GPS antennas, which are required to accept radiation from multiple directions simultaneously. These errors affect estimates of all parameters that are estimated from the GPS phase data, including site position (and hence velocity) and the neutral atmospheric and ionospheric propagation delays.

A number of studies have been conducted to address these types of errors. The earliest modeling studies [e.g., *Young et al.*, 1985; *Georgiadou and Kleusberg*, 1988] were based on reflection from a simple horizontal ground surface. *Elosegui et al.* [1995] found that these simple models worked fairly well for near-field signal scattering as well. Such simple models cannot, though, capture the unique and complex geometry at each GPS site, though they seem to be useful for the largest multipath errors (4-5 mm of phase or more for L1 [*Elosegui et al.*, 1995]). *Axelrad et al.* [1996] developed a method for inferring multipath from recorded signal-to-noise ratio (SNR) variations. This approach seems to be limited by the accuracy of the SNR determinations, however.

Anechoic chamber measurements of GPS antenna phase patterns [*Schupler et al.*, 1994] indicate contributions of up to ~20 mm with variation of azimuth and elevation. However, these measurements are of limited use because of the near-field nature of the problem [*Elosegui et al.*, 1995]. In the field, GPS antennas are usually directly mounted on larger structures that electromagnetically couple to the antenna, effectively modifying the phase pattern. Some improvements have been noted with corrections based on anechoic chamber measurements, but such corrections cannot deal with site variations. This same problem applies to the mapping of phase-center variations in the field using a robot that rotates the

antenna about several axes [*Wubben et al.*, 2000]. Indeed, the robot itself may become coupled electromagnetically to the GPS antenna during calibration.

An entirely ad hoc approach capitalizes on the assumed repeatability of these effects [e.g., *Genrich and Bock*, 1992; *Bock et al.*, 2000]. The GPS constellation is in a pseudosynchronous orbit, with the topocentric satellite positions repeating every sidereal day. *Bock et al.* [2000] have filtered out the common mode effects of signal multipath using the sidereal repetition. Even though this method is very effective and computationally efficient, it also can filter out other signals that have sidereal periods. Another disadvantage of this correction is that it is based on post-processing analysis. Thus, multipath errors at each individual site might have already propagated into the estimates of other parameters, especially in the vertical position estimate.

Despite these studies, a great deal regarding these important error sources remains uncertain, including their variability with site and over time. This latter effect can be expected since sites physically change over time, both seasonally (e.g., foliage changes) and on shorter time scales (moisture and precipitation, and equipment changes). What is required is an *in situ* method for measuring these effects. With that goal, we have developed an Antenna and Multipath Calibration System (AMCS) that uses a relatively high gain parabolic antenna to calibrate a GPS antenna at a site. The parabolic antenna is directional and suffers from negligible phase-center variations and multipath.

In this article, we describe the design and operational aspects of the AMCS. We also present preliminary tests designed to assess the system accuracy of the AMCS. We present evidence that the AMCS can measure combined multipath and phase-center effects with an accuracy of about ~1 mm (at L1). Our initial measurements indicate a greater directional variability and higher sensitivity to environmental conditions than that indicated by previous studies.

ELEMENTS OF THE AMCS

The AMCS system has been constructed at the MIT Haystack Observatory in Westford, Massachusetts. The AMCS consists mainly of two Trimble 4000 SSI receivers and a parabolic antenna (refer to Figure 1).

Both receivers are connected to a 5 MHz signal derived from the Hydrogen Maser located at the Haystack Observatory. The Allan standard deviation of the H maser is 10^{-14} s $^{-1}$ for periods between 10 and 10^5 seconds.

However, this level of high accuracy clock source is not a must for the system.

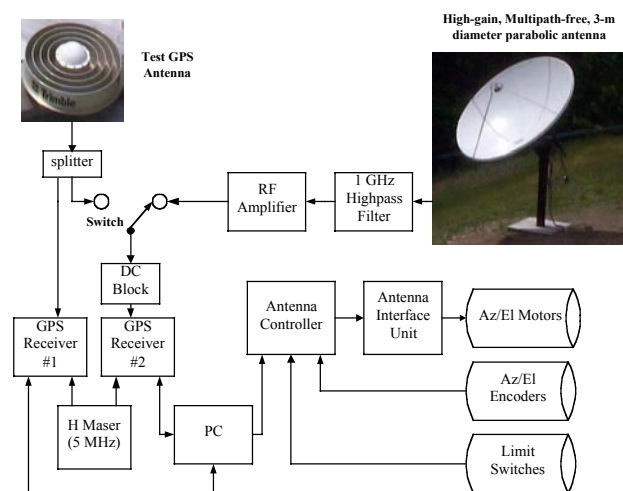
To calibrate the receiver synchronization error, we have found it useful to be able to operate in a “zero baseline” (ZBL) mode, in which both receivers are connected to the test antenna. We have therefore connected a splitter to the cable from the test antenna and a switch enables us to choose between this ZBL mode and “AMCS mode,” in which GPS receiver #1 is connected to the parabolic antenna (Figure 1).

One Trimble receiver is always connected to the test antenna, but the other receiver can receive the GPS signal either from the test antenna or the parabolic antenna. A GPS antenna splitter is connected to the test antenna so that it can feed the received signal simultaneously to the two receivers. This is the case for the ZBL mode data processing where two receivers record the same signal received at the test antenna, fed by the splitter. When a single GPS antenna is connected to two receivers, a DC block is needed in one of the lines; otherwise both receivers would be trying to feed DC power to the antenna. In the AMCS system, there is a DC block between the switch output and the receiver connected to it (refer to Figure 1).

Figure 1. The AMCS block diagram

The interface to the receivers and the antenna controller is handled by a PC, which is equipped with Pentium III processor at 450 MHz and 96MB 100MHz SDRAM. The operating system is Windows 98. The interface and control package was developed using LabVIEW and MATLAB.

The Parabolic Antenna



Andersen Manufacturing Inc. manufactured the 3.0-meter hydroformed aluminum parabolic reflector antenna. It has a prime-focus feed support structure, elevation-over-

azimuth dual-axis motion, and DC electric motor drives on both axes (Figure 1). The paraboloid antenna can be pointed in directions within the ranges of 7°-357° in azimuth and 5°-87° in elevation. The tracking precision is around 0.1° in the elevation direction and 0.5° in the azimuth direction. The azimuth drive has a speed of 2.0 °/s and the elevation drive a speed of 0.8°/s. The antenna was mounted on a vertical 20-cm-diameter, 3-m-long steel pipe anchored in a concrete block with dimensions 1.2× 1.2 × 1.2 m.

Control of the parabolic antenna is provided by a Research Concepts model RC2500 satellite antenna controller. Antenna position is sensed in both axes with 12-bit Clifton Precision angle resolvers, which have 6' resolution. The digital output from each resolver is fed to the controller, which compares the antenna position against the commanded position. If the position difference is larger than a pre-set threshold for either axis, the controller enables the appropriate open collector output lines to two Research Concepts antenna interface units, one for each axis. These units supply 36 VDC of the proper sign to the antenna motors to drive the antenna to the commanded position. Remote monitor and control of the RS2500 is available via an RS422 link.

In deciding what direction to drive a motor when a change in azimuth is requested, the RC2500 does not recognize that 0° and 360° are the same direction. Therefore, if the new azimuth has a lower (higher) numerical value, the motor will drive the antenna in a CCW (CW) direction, without ever passing through 0° azimuth. Mechanical limit switches were installed to prevent the paraboloid antenna from passing through the 360° point in the azimuthal direction and the 0° or 90° point in the elevation direction. For redundancy, limits were hard-coded in the antenna control software. The mechanical limits are 358.6° in azimuth (moving CW), 4.6° in azimuth (moving CCW), 89.0° in elevation (moving upward), and -0.5° in elevation (moving downward). The software limits are 357.0° in azimuth (CW), 7.0° in azimuth (CCW), 87.0° in elevation (up), and 4.8° in elevation (down).

The phase-stabilized version of Andrew FSJ1 50A cable is used to carry the RF signal from the parabolic antenna feed to the Trimble receiver. The attenuation at the L1 and L2 frequencies over the 30-m length of the cable is approximately 7 dB. The temperature sensitivity of the electrical length of the cable varies from -0.2 to +0.3 mm/deg C over the temperature range -30 to +40 °C.

The parabolic antenna system has a 3-dB beamwidth of ~4.5° at L1 and 6° at L2 and is primarily sensitive to RCP signals. The antenna feed, manufactured by Microwave Engineering, receives LCP (into which RCP is converted

by the primary antenna reflector) with an axial ratio of <3 dB at L1 and L2 over all angles subtended by the primary reflector.

Operation and Interface

The LabVIEW graphical user interface is used to create and run the automatic scheduler, and to operate the AMCS manually. The mode can be switched between ZBL and AMCS, the satellites to be observed can be selected, the antenna pointed, and the observation logging started and stopped. The LabVIEW routines also control the communication between the PC and the GPS receivers. The multiple receiver channels can be assigned to specific satellites, and the satellite ephemerides and phase data downloaded. Figure 2 shows the main AMCS graphical interface.

The LabVIEW routines are supported by a set of

MATLAB routines that handle computationally more intensive tasks, such as calculation of topocentric satellite positions, least-squares solution for synchronization errors, and calibration solutions.

With an Internet connection, we can remotely operate the AMCS. Timbuktu Pro 32 (version 2.0, 32-bit; Netopia Inc.) was used for remote control of the system. This software allows one to access necessary files on the PC and run every program on it. For safety reasons, a Logitech QuickCam camera was connected to the PC so that one can remotely observe the parabolic antenna while the main program is controlling the parabola.

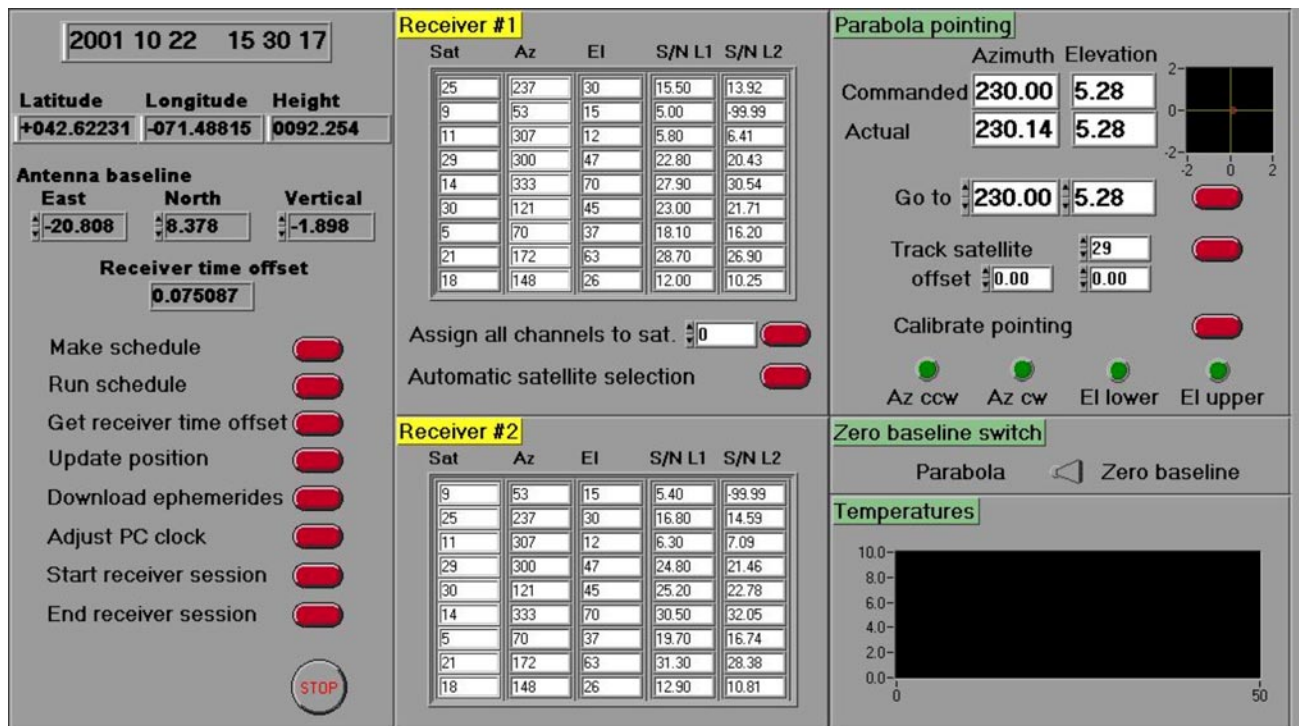


Figure 2. The first interactive window of the main AMCS program

ANALYSIS OF RECEIVER ERRORS

To evaluate the contribution of receiver noise, we examine post-fit phase residuals from ZBL observations. In ZBL mode, two receivers simultaneously record the signal from the test antenna. Thus, the baseline length between two antennas is zero. In this mode, one can determine the synchronization error and the phase offsets for each satellite. For such observations, many of the terms in the carrier phase observation equation are zero, leaving us with the simplified ZBL model:

$$\Delta\phi^k(t) = \frac{f}{c} \dot{\rho}(t)\Delta T + \Delta\phi_o^k, \quad (1)$$

where $\Delta\phi^k$ is the differenced phase for the satellite k , f is the frequency, c is the speed of light, $\dot{\rho}$ is the range rate, ΔT is the clock synchronization error, and $\Delta\phi_o^k$ is the phase offset for the satellite k . The GPS phase is often expressed in units of length, i.e., the terms in Equation (1) multiplied by the wavelength of ~ 0.19 m for L1 and ~ 0.24 m for L2. For the following, we show results for L1 only. Noise values for L2 can be expected to scale by the ratio of the wavelengths.

The model for the AMCS-mode phase difference is:

$$\Delta\varphi^k(t) = \dot{\rho}(t)\Delta\hat{T} + \Delta\hat{\phi}_o^k + \lambda N + \vec{s} \cdot \vec{b} + C \cos \varepsilon, \quad (2)$$

where $\Delta\hat{T}$ and $\Delta\hat{\phi}_o^k$ denote the estimated values of the receiver clock synchronization error and phase offsets in the ZBL-mode analysis. These estimated values are used in the AMCS-mode analysis as constants. In Equation (2), λ is the wavelength, N is the integer ambiguity, \vec{s} is the satellite topocentric vector, and \vec{b} is the baseline vector between two antenna reference points (denoted as red dots in Figure 3). C is the length of the azimuth arm of the parabolic antenna as shown in Figure 3 and ε is the elevation angle of the GPS satellite. The phase φ in Equation 2 is in meters, whereas ϕ in Equation 1 is in cycles.

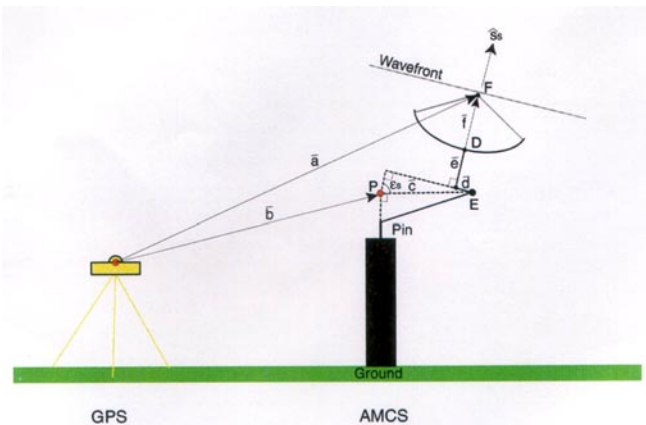


Figure 3. Schematic Diagram of the AMCS

We present the analysis of a typical ZBL L1 data set in Figure 4, where five GPS satellites were observed for the 10-minute data logging session. A typical ZBL calibration run consists of ten minutes of multi-channel, multi-satellite data set. For each 10-minute run with N satellites, we estimate $N + 1$ parameters: ΔT and $\Delta\phi_o^k$, $k = 1, \dots, N$. Observations are acquired every 10 seconds, so the approximate number of ZBL observations is $60 \times N$ (The Trimble 4000 SSI can observe up to 9 satellites simultaneously, but usually only 6-8 are visible.) The RMS of phase residuals for the data set in Figure 4 is 0.54 mm. Typical RMS accuracies of ZBL-mode phase residuals are sub-millimeter, in the ranges of 0.4-0.7 mm for L1.

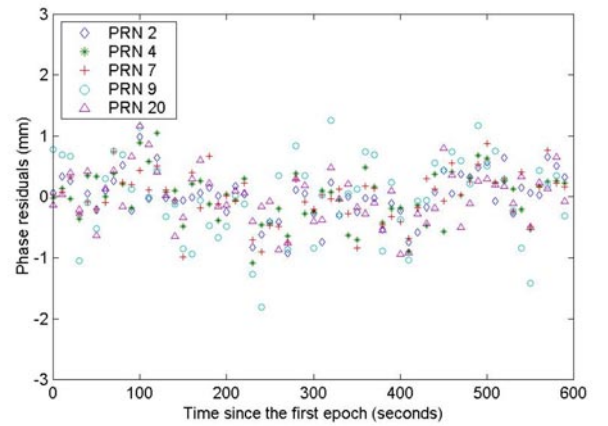


Figure 4. An example of L1 phase residuals for ZBL mode

DETERMINATION OF ANTENNA AND MULTIPATH CALIBRATION ERRORS

In this section, we present tracking-parabola AMCS-mode tests. In the AMCS-mode data collection, one GPS receiver records the signal received at the test antenna, and the other records the signal from the parabolic antenna. In this analysis, one can compare the phase data from the two receivers. With this approach, we were able to obtain the multipath signals. We programmed the AMCS so that the parabolic antenna follows the target GPS satellite. We collected 10 minutes of ZBL data, followed by 15 minutes of tracking data. As in the earlier test, the receiver clock synchronization error and phase offsets for each satellite obtained in ZBL data analysis were used in AMCS data processing as constants. We tested with a variety of configurations by tracking different GPS satellites and using low-, medium-, and high- elevation angles.

Figure 5 shows phase residuals of PRN 1 for four

consecutive days (November 18-21, 2001). We sampled the phase residual at every 10 seconds, and smoothed them using the 50-second boxcar filtering. For the tracking period of 15 minutes, the elevation angle varied 6° (20.0° to 26.0°), but the azimuth angle changed only 1° (310.2° to 311.2°). We see that the phase residuals repeat very nicely for four consecutive days. Considering slightly different weather conditions for four days of experiment, this level of repetition implies that the observed repeating pattern is highly dependent on the satellite geometry. Part of this might be caused by the antenna phase center variations. However, the test antenna is equipped with choke rings and an antenna with choke rings does not show this level of amplitude variations depending on the satellite geometry. Thus, we conclude the repeating pattern of phase residuals observed in Figure 5 is the multipath.

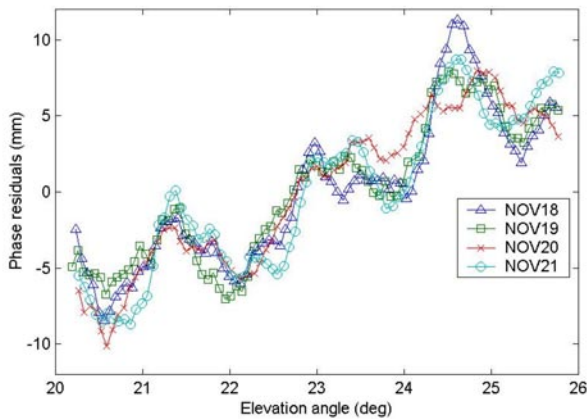


Figure 5. Repeating phase residuals from GPS PRN 1 for four consecutive days

We repeated the same experiment with different satellites and various azimuth and elevation angle configurations. Without regard to the satellite or elevation and azimuth angles, the phase residuals repeat daily in all cases. The RMS of daily differences was at ~ 1 mm level. The amplitude of the variations is 4-7 mm for low elevation angles and 1-2 mm for high elevation angles. The RMS of phase residuals is up to several millimeters. However, we could model the variations of the phase residuals using a simple boxcar filtering. After the modeled repeating

patterns were subtracted from the raw residuals, the RMS was reduced down to ~ 1 mm.

We see that the multipath changes very rapidly with the elevation angle. For example, Figure 5 shows that the observed signal has a period of 1.5° in the elevation angle. This level of high frequency multipath signal was not reported in the literature before.

To verify that the repeating pattern of signals observed at the first test antenna is truly multipath, we decided to install another test GPS antenna in a low multipath environment so that we can compare the signals obtained at each antenna. The second antenna is also a choke ring antenna manufactured by Trimble, which is the same type as the first one. We have installed the second GPS antenna nearby the first antenna. The second antenna is located where the multipath effects are presumably less significant than at the location of the first antenna. It is surrounded by all-weather microwave absorbers to further reduce multipath effects.

We have collected data for seven days in February 2002. Because AMCS is set up to calibrate one test antenna at a time, we switched back and forth between two test antennas. The first test antenna was used for five days (February 13, 15, 17, 19, and 20) and the second for two days (February 16 and 18). As in the previous tracking tests, the parabolic antenna was tracking each GPS satellite for 15 minutes, preceded by 10 minutes of ZBL. Figure 6 shows phase residuals from each antenna. In (a) and (b) of Figure 6, the phase residuals nicely repeat for the first test antenna and the amplitude of the antenna is 7-8 mm. In the third case of the first antenna (c), the residuals don't repeat as nicely as the first two cases, but they are quite correlated and the amplitude (only 1-2 mm) is significantly smaller than (a) and (b). The observed lower amplitude of (c) was expected because (a) and (b) are for low elevation angles, where the multipath effect are one of the most dominant error sources in GPS measurements. The errors due the atmosphere are also significant in the low elevation angles, but they do not repeat daily. If we compare the pairs of (a)-(d), (b)-(e), and (c)-(f), each GPS satellite was passing through the same part of the sky for seven days.

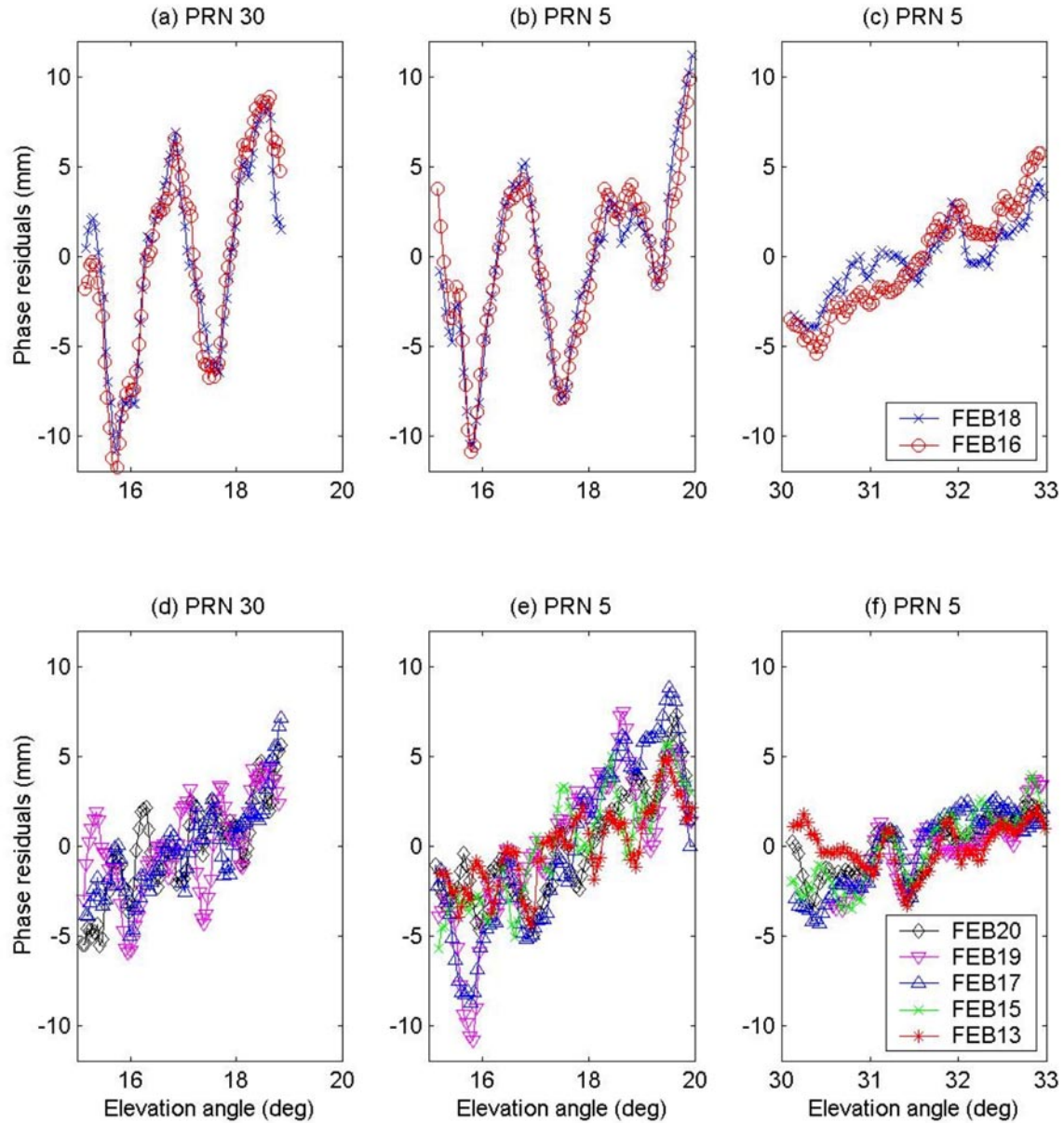


Figure 6. Phase residuals from two test antennas. Tracking GPS PRN 30 in low elevation angles and phase residuals (in mm) at the first antenna (a) and the second antenna (d). Tracking GPS PRN5 in low elevation angles and phase residuals (in mm) at the first antenna (b) and the second antenna (e). Tracking GPS PRN 5 in medium elevation angles and phase residuals (in mm) at the first antenna (c) and the second antenna (f).

The only temporal difference for those seven days is that it takes a sidereal day (which is 236 seconds shorter than a solar day) for the target GPS satellite comes back to the same location where it was one day earlier. Even though the AMCS was observing the same satellite with the same satellite geometry, the signals observed at each antenna is totally different. The fact that the signals recorded at the second test antenna is of smaller amplitudes and non-repeatable implies that the signal observed at the first

antenna is truly the multipath.

The repeating patterns of the residuals in (a) and (b) are very similar. The reason is because PRN 30 and 5 pass almost the same part of sky. The elevation angle of PRN 30 changes from 15° to 19°, whereas the PRN 5 from 15° to 20°. The azimuth angles are also very close to each other; PRN 30 changes from 318.5° to 313.8° and PRN 5 from 317.8° to 314.8°. Thus, PRN 30 moves a little faster

than PRN 5 in the azimuthal direction but slower in the elevation direction. However, they are never separated more than 1° in either direction.

For each set of Figure 5, the residuals at the second test antenna do not repeat as nicely as at the first antenna, which is not surprising because the second antenna is in low multipath environment. The amplitude of the signal is also significantly smaller than at the first antenna. However, from (f), we see perfectly repeating patterns around 31° , which might be due to an outstanding multipath source.

ACKNOWLEDGEMENTS

We thank MIT Haystack Observatory for hosting the AMCS. We thank Mark Derome, Bruce Whittier, and Ken Wilson for their major contributions to the construction and maintenance of the AMCS.

REFERENCES

Axelrad, P., C. J. Comp, and P. F. MacDoran, SNR based multipath error correction for GPS differential phase, *IEEE Trans. on Aerospace and Electronic Systems*, 32(2), 650–660, April 1996

Bock, Y., R. M. Nikolaidis, P. J. de Jonge, and M. Bevis, Instantaneous geodetic positioning at medium distances with the Global Positioning System, *J. Geophys. Res.*, 105(B12), 28,223–28,253, December 2000

Byun, S. H., G. A. Hajj, and L. E. Young, Assessment of GPS signal multipath interference, *Proceedings of ION National Technical Meeting*, San Diego, CA., January 28-30, 2002

Elosegui, P., J. L. Davis, R. T. K. Jaldehag, J. M. Johansson, A. E. Niell, and I. I. Shapiro, Geodesy using the Global Positioning System: The effects of signal scattering on estimates of site position, *J. Geophys. Res.*, 100(B7), 9921–9934, June 1995

Genrich, J. F. and Y. Bock, Rapid resolution of crustal motion at short ranges with Global Positioning System, *J. Geophys. Res.*, 97(B3), 3261–3269, March 1992

Georgiadou, Y. and A. Kleusberg, On carrier signal multipath effects in relative GPS positioning, *Manuscripta Geodaetica*, 13, 172–179, 1988

Mader, G. L. and J. R. MacKay, Calibration of GPS antennas, In *Proceedings of the IGS 1996 Analysis Center Workshop*, Pasadena, CA, 81–106, March 1996

Rothacher M., S. Schaer, L. Mervart, and G. Beutler, Determination of antenna phase center variations using GPS data, *IGS Workshop Proceedings: Special Topics and New Directions*, Potsdam, Germany, 205–220, May

15-17, 1995

Segall, P. and J. L. Davis, GPS applications for geodynamics and earthquake studies, *Annu. Rev. Earth Planet. Sci.*, 25, 301–336, 1997

Schupler, B. R., R. L. Allshouse, and T. A. Clark, Signal characteristics of GPS user antennas, *Navigation: Journal of The Institute of Navigation*, 41(3), 277–295, Fall 1994

Wubben G., M. Schmitz, F. Menge, V. Boder, and G. Seeber, Automated absolute field calibration of GPS antennas in real-time, *Proceedings of the ION GPS-2000 13th International Technical Meeting of The Satellite Division of The Institute of Navigation*, Salt Lake City, 2000

Young, L. E., R. E. Neilan, and F. R. Bletzacker, GPS satellite multipath: An experimental investigation, *Proceedings of the First Symposium on Precise Positioning with the Global Positioning System*, 423–432, National Oceanic and Atmospheric Administration, Rockville, Maryland, 1985